# Label-Free DNA Detection of Hepatitis C Virus Based on Modified Conducting Polypyrrole Films at Microelectrodes and Atomic Force Microscopy Tip-Integrated Electrodes

**ARTICLE** *in* ANALYTICAL CHEMISTRY · FEBRUARY 2008

Impact Factor: 5.64 · DOI: 10.1021/ac701613t · Source: PubMed



**6 AUTHORS**, INCLUDING:

Christine Kranz
Universität Ulm
**129** PUBLICATIONS **2,418** CITATIONS
SEE PROFILE

Hideko Yamanaka
São Paulo State University
**64** PUBLICATIONS **759** CITATIONS
SEE PROFILE

Boris Mizaikoff
Universität Ulm
**309** PUBLICATIONS **4,784** CITATIONS
SEE PROFILE

Mira Josowicz
Georgia Institute of Technology
**117** PUBLICATIONS **3,557** CITATIONS
SEE PROFILE

*Anal. Chem.* **2008,** *80,* 237−245

# Label-Free DNA Detection of Hepatitis C Virus Based on Modified Conducting Polypyrrole Films at Microelectrodes and Atomic Force Microscopy Tip-Integrated Electrodes

**Carla dos Santos Riccardi,[†] Christine Kranz,*[,†] Janusz Kowalik,[†] Hideko Yamanaka,[‡] Boris Mizaikoff,[†] and Mira Josowicz*[,†]**

*School of Chemistry and Biochemistry, Georgia Institute of Technology, 901 Atlantic Dr, Atlanta, Georgia 30332-0400, and Unesp-Universidade Estadual Paulista, Instituto de Química de Araraquara, R. Prof. Francisco Degni, s/n R. Prof. Francisco Degni s/n 14800-900 Araraquara, SP, Brazil*

**We present a new strategy for the label-free electrochemical detection of DNA hybridization for detecting hepatitis C virus based on electrostatic modulation of the ion-exchange kinetics of a polypyrrole film deposited at microelectrodes. Synthetic single-stranded 18-mer HCV genotype-1-specific probe DNA has been immobilized at a 2,5-bis(2-thienyl)-*N*-(3-phosphoryl-*n*-alkyl)pyrrole film established by electropolymerization at the previously formed polypyrrole layer. HCV DNA sequences (244-mer) resulting from the reverse transcriptase-linked polymerase chain reaction amplification of the original viral RNA were monitored by affecting the ion-exchange properties of the polypyrrole film. The performance of this miniaturized DNA sensor system was studied in respect to selectivity, sensitivity, and reproducibility. The limit of detection was determined at $1.82 \times 10^{-21}$ mol $L^{-1}$. Control experiments were performed with cDNA from HCV genotypes 2a/c, 2b, and 3 and did not show any unspecific binding. Additionally, the influence of the spacer length of 2,5-bis(2-thienyl)-*N*-(3-phosphoryl-*n*-alkyl)pyrrole on the behavior of the DNA sensor was investigated. This biosensing scheme was finally extended to the electrochemical detection of DNA at submicrometer-sized DNA biosensors integrated into bifunctional atomic force scanning electrochemical microscopy probes. The 18-mer DNA target was again monitored by following the ion-exchange properties of the polypyrrole film. Control experiments were performed with 12-base pair mismatched sequences.**

The hepatitis C virus (HCV) is responsible for most of the cases of post-transfusion non-A and non-B hepatitis.[1] The infection affects ∼170 million individuals worldwide.[2] The major causes of HCV infection worldwide are organ transplantation, blood transfusions, renal dialysis, and intravenous drug abuse.[3] HCV is a positive-sense, single-stranded RNA virus that displays extensive genetic heterogeneity. At present, 11 types and 70 subtypes of the virus have been discriminated.[4]

Laboratory diagnosis and monitoring of viral hepatitis are important research areas in the infectious pathology of the liver. An important task during clinical laboratory diagnosis is the detection of HCV RNA levels (viral load) and of HCV genotype information. Monitoring of HCV RNA in serum or plasma is an indication for diagnosing or confirming active infections and for assessing the patient response to therapy.[5]

A variety of commercial assays have been developed for the qualitative detection of HCV RNA based on different nucleic acid amplification methodologies such as, for example, reverse transcription and polymerase chain reaction (RT-PCR), transcription-mediated amplification, and nucleic acid sequence-based amplification.[6] The commercial tests available for qualitative detection of HCV RNA are based on electrochemiluminescence measurements detecting the amplified RNA product by using a target-specific capture probe bound to magnetic particles in conjunction with a ruthenium-labeled detection probe.[7] HCV RNA qualitative spectrophotometric detection by Amplicor HCV (Roche, USA) offers the detection of HCV RNA levels as low as 50 IU/mL.[8] Clinically used tests for detecting HCV RNA are based on either

* To whom correspondence should be addressed. Fax: 404-894-7452. E-mail: christine.kranz@chemistry.gatech.edu; mira.josowicz@chemistry.gatech.edu.
[†] Georgia Institute of Technology.
[‡] Unesp-Universidade Estadual Paulista.

(1) Touzet, S.; Kraemer, L.; Colin, C.; Pradat, P.; Lanoir, D.; Bailly, F.; Coppola, R. C.; Sauleda, S.; Thursz, M. R.; Tillmann, H.; Alberti, A.; Braconier, J. H.; Esteban, J. I.; Hadziyannis, S. J.; Manns, M. P.; Saracco, G.; Thomas, H. C.; Trepo, C. *Eur. J. Gastroenterol. Hepatol.* **2000**, *12*, 667−678.
(2) Hofmann, W. P.; Dries, V.; Herrmann, E.; Gartner, B.; Zeuzem, S.; Sarrazin, C. *J. Clin. Virol.* **2005**, *32*, 289−293.
(3) WHO Consultation. *J. Viral Hepatol.* **1999**, *6*, 35−47.
(4) Simmonds, P.; Alberti, A.; Alter, H. J.; Bonino, F.; Bradley, D. W.; Brechot, C.; Brouwer, J. T.; Chan, S. W.; Chayama, K.; Chen, D. S.; et al. *Hepatology* **1994**, *19*, 1321−1324.
(5) Consensus Statement. *J. Hepatol.* **1999**, *30*, 956−961.
(6) (a) Erensoy, S. *J. Clin. Virol.* **2001**, *21*, 271−281. (b) Novati, R.; Thiers, V.; Monforte, A.; Maisonneuve, P.; Principi, N.; Conti, M.; Lazzarin, A.; Brechot, C. *J. Infect. Dis.* **1992**, *165*, 720−723. (c) Hollingsworth, R. C.; Sillekens, P.; VanDeursen, P.; Neal, K. R.; Irving, W. L. *J. Hepatol.* **1996**, *25*, 301−306. (d) Damen, M.; Sillekens, P.; Cuypers, H. T. M.; Frantzen, I.; Melsert, R. *J. Virol. Methods* **1999**, *82*, 45. (e) Lee, S. C.; Antony, A.; Lee, N.; Leibow, J.; Yang, Q. J.; Soviero, S.; Gutekunst, K.; Rosenstraus, M. *J. Clin. Microbiol.* **2000**, *38*, 4171−4179.
(7) Guichon, A.; Chiaprelli, H.; Martinez, A.; Rodrigues, C.; Trento, A.; Russi, C. J.; Carballal, G. *J. Clin. Virol.* **2004**, *29*, 84−91.

10.1021/ac701613t CCC: $40.75 
Published on Web 11/23/2007

qualitative (PCR, Amplicor HCV v2.0 Roche Molecular Systems; or transcription-mediated amplification, Versant HCV RNA Bayer Diagnostics) or quantitative (PCR, LCx HCV RNA Abbott Diagnostics, SuperQuant National Genetics Institute, Amplicor HCV Monitor v2.0 Roche Molecular Systems and Cobas Amplicor HCV Monitor Roche Molecular Systems, or Branched DNA: Versant HCV RNA 3.0 Bayer Diagnostics) approaches.[9] Furthermore, in addition to the viral load, HCV genotyping is important for predicting HCV medical treatment response and treatment duration. Several methods for genotyping HCV have been developed, including direct DNA sequencing, type-specific PCR, restriction fragment length polymorphism, line probe assays, primer-specific and mispair extension analysis, heteroduplex mobility analysis by temperature gradient capillary electrophoresis, and denaturing high-performance liquid chromatography. Nucleotide sequence analysis is the reference method for identifying different genotypes of HCV. However, because this method is expensive, time-consuming, and requires special equipment for sequencing, it has been restricted to research settings and is considered impractical for large-scale clinical studies.[10]

Furthermore, biosensor devices for the qualitative and quantitative detection of HCV by bioelectric recognition assays,[11] surface plasmon resonance (BIAcore),[12] and piezoelectric response[13] have been published. Biosensors based on conducting polymers have been successfully applied to the genotyping of HCV in blood samples by fluorescence detection.[14] Several papers have been published on electrochemical genosensors for hepatitis B virus;[15] however, to date little is reported on RNA HCV detection.[16]

The development of electrochemical DNA biosensors combining base pair recognition of DNA probes with a miniaturized sensing platform has received increasing attention.[17] Methods for anchoring probe oligonucleotides to the transducer rely on the availability of functional groups at the transducer surface. Recently, we described a label-free detection scheme for short-sequence (18- and 27-mer) DNA based on conducting modified polypyrrole films deposited at a microelectrode surface.[18] Thompson et al. described the fundamental detection scheme of this approach based on a bilayer with phosphonic acid tethers for DNA immobilization at electrode surfaces.[19]

Within the present study, we extend the application of this label-free electrochemical detection method to qualitative HCV RNA detection and genotyping based on electrostatic modulation of the ion-exchange kinetics of a polypyrrole film. Synthetic single-stranded, 18-mer oligonucleotide probes (5′-CGC TCA ATG CCT GGA GAT-3′) have been immobilized at 2,5-bis(2-thienyl)-*N*-(3-phosphoryl-*n*-alkyl)pyrrole with different alkyl chain length <pTPT**C3**-$PO_3H_2$> or <pTPTC**11**-$PO_3H_2$>; films were formed by electropolymerization at a previously deposited polypyrrole layer. The complementary DNA strand (244-mer cDNA from HCV genotype 1) obtained by RT-PCR was monitored via the ion-exchange properties of the polypyrrole film. The influence of an extended spacer length, which increases the steric flexibility and distance between the biosensor surface and the probe DNA sequence, on the hybridization efficiency was also investigated. The performance of the miniaturized DNA sensor system was studied in respect to selectivity, sensitivity, and reproducibility. Further miniaturization to submicrometer DNA electrodes could be achieved by modifiying an AFM tip-integrated electrode as described above. Synthetic single-stranded 18-mer HCV-1 DNA probe (5′-CGC TCA ATG CCT GGA GAT-3′) has been immobilized at 2,5-bis(2-thienyl)-*N*-(3-phosphorylpropyl)pyrrole <pTPT**C3**-$PO_3H_2$> films, and a short-sequence DNA target (18-mer: 5′-ATC TCC AGG CAT TGA GCG-3′) was monitored via modulation of the ion-exchange properties of the polypyrrole film. Control experiments were performed with a 12-base mismatched sequence (5′-CAC TCT ATG TCC GGT CAT-3′). In addition, a miniaturized DNA sensor was positioned using scanning electrochemical microscopy (SECM) with a dual microdisk electrode.[20] One disk of the electrode assembly was modified with the DNA sensing layer, while the second electrode was used for positioning.[21] After the sensor was positioned in proximity to the sample surface, oligonucleotide target DNA (18-mer) was detected after diffusion through a porous polycarbonate membrane mimicking a localized DNA source.

## EXPERIMENTAL SECTION

**Chemicals.** Pyrrole monomer (Py, 98%) was purchased from Sigma-Aldrich (St. Louis, MO). Prior to use, pyrrole was purified by passing it through a neutral alumina column. 2,5-Bis(2-thienyl)-*N*-(3-phosphoryl-*n*-alkyl)pyrrole (pTPTC*n*-$PO_3H_2$, $n = 3$ or 11) is not commercially available and was synthesized according to Hartung et al. .[22] Magnesium chloride was obtained from Fluka. Tetra-*n*-butylammonium perchlorate was obtained from Alfa Aesar (Ward Hill, MA). All other reagents were obtained from Sigma-Aldrich and were used without further purification. Tris-


(8) Roche-diagnostics. Retrieved 06 November 2005 <http://www.roche-diagnostics.com>.
(9) William-Carey, M. D. *Clin. J. Med.* **2003**, *70*, S7−S13.
(10) Antonishyn, N. A.; Ast, V. M.; McDonald, R. R.; Chaudhary, R. K.; Lin, L.; Andonov, A. P.; Horsman, G. B. *J. Clin. Microbiol.* **2005**, *43*, 5158−5163.
(11) Kintzios, S.; Pistola, E.; Konstas, J.; Bem, F.; Matakiadis, T.; Alexandropoulos, N.; Biselis, I.; Levin, R. *Biosens. Bioelectron.* **2001**, *16*, 467.
(12) (a) Richalet-Secordel, P. M.; Poisson, F.; VanRegenmortel, M. H. V. *Clin. Diagn. Virol.* **1996**, *5*, 111−119. (b) O'Meara, D.; Yun, Z. B.; Sonnerborg, A.; Lundeberg, J. *J. Clin. Microbiol.* **1998**, *36*, 2454−2459.
(13) Skládal, P.; Riccardi, C. S.; Yamanaka, H.; da Costa, P. I. *J. Virol. Methods* **2004**, *117*, 145−151.
(14) Bidan, G.; Billon, M.; Livache, T.; Mathis, G.; Roget, A.; Torres-Rodriguez, L. M. *Synth. Met.* **1999**, *102*, 1363−1365.
(15) (a) Zhao, H. T.; Ju, H. X. *Electroanal.* **2004**, *16*, 1642−1646. (b) Kobayashi, M.; Takashi, K. B.; Saito, M.; Kaji, S.; Oomura, M.; Iwabuchi, S.; Morita, Y.; Hasan, O.; Tamiya, E. *Electrochem. Commun.* **2004**, *6*, 337−343. (c) Ye, T. K.; Zhao, J. H.; Yan, F.; Zhu, Y. L.; Ju, H. X. *Biosens. Bioelectron.* **2003**, *18*, 1501−1508. (d) Ju, H. X.; Ye, Y. K.; Zhao, J. H.; Zhu, Y. L. *Anal. Biochem.* **2003**, *313*, 255−261. (e) Meric, B.; Kerman, K.; Ozkan, D.; Kara, P.; Erensoy, S.; Akarca, U. S.; Mascini, M.; Ozsoz, M. *Talanta* **2002**, *56*, 837−846. (f) Xu, D. K.; Huang, K.; Liu, Z. H.; Liu, Y. Q.; Ma, L. R. *Electroanalysis* **2001**, *13*, 882−887. (g) Erdem, A.; Kerman, K.; Meric, B.; Akarca, U. S.; Ozsoz, M. *Anal. Chim. Acta* **2000**, *422*, 139−149. (h) Erdem, A.; Kerman, K.; Meric, B.; Akarca, U. S.; Ozsoz, M. *Electroanalysis* **1999**, *11*, 586−588. (i) Hashimoto, K.; Ito, K.; Ishimori, Y. *Sens. Actuators, B* **1998**, *46*, 220.
(16) Riccardi, C. S.; Dahmouche, K.; Santilli, C. V.; da Costa, P. I.; Yamanaka, H. *Talanta* **2006**, 7, 637−643.
(17) Kerman, K.; Kobayashi, M.; Tamiya, E. *Meas. Sci. Technol.* **2004**, *15*, R1−R11.
(18) Riccardi, C. S.; Yamanaka, H.; Josowicz, M.; Kowalik, J.; Mizaikoff, B.; Kranz, C. *Anal. Chem.* **2006**, *78*, 1139−1145.
(19) Thompson, L. A.; Kowalik, J.; Josowicz, M.; Janata, J. *J. Am. Chem. Soc.* **2003**, *125*, 324−325.
(20) (a) Bard, A. J.; Fan, F. R. F.; Mirkin, M. V. *Electroanal. Chem.* **1994**, *18*, 243−373. (b) Yasukawa, T.; Kaya, T.; Matsue, T. *Anal. Chem.* **1999**, *71*, 4637−4641. (c) Wei, C.; Bard, A. J.; Nagy, G.; Toth, K. *Anal. Chem.* **1995**, *67*, 1346−1356.
(21) Kueng, A.; Kranz, C.; Mizaikoff, B. *Biosens. Bioelectron.* **2005**, *21*, 346−353.

**Table 1. Investigated Oligonucleotide Sequences**

| description | sequence |
|---|---|
| 18-mer DNA probe (HCV-1) | 5′-CGC TCA ATG CCT GGA GAT-3′ |
| 18-mer DNA target (HCV-1) | 5′-ATC TCC AGG CAT TGA GCG-3′ |
| 18-mer mismatched DNA | 5′-**CA**C TC**T** AT**G** **TCC** **GGT** **CAT**−3′ |
| 244-mer DNA target (HCV-1) | 5′-ATC TCC AGG CAT TGA GCG-3′ |
| 244-mer DNA (HCV-2a/c) | 5′-AT**G** **G**CC **G**GG CAT **A**GA G**T**G-3′ |
| 244-mer DNA (HCV-2b) | 5′-AT**G** **A**CC **GGA** CAT **A**GA G**T**G-3′ |
| 244-mer DNA (HCV-3) | 5′-AT**T** TC**T** **G**GG **T**AT TGA GCG-3′ |

**Table 2. Total Charge Supplied by the Electrode for the Polymerization of PPy and pTPTC*n*-$PO_3H_2$ on the Different Electrode Surfaces**

| electrode | $A$/cm$^2$ | PPy charge/C | pTPTC*n*-$PO_3H_2$ charge/C |
|---|---|---|---|
| 10-$\mu$m Pt dual microdisk electrode | $7.90 \times 10^{-7}$ | $1.60 \times 10^{-7}$ | $1.3 \times 10^{-7}$ |
| 25-$\mu$m Pt microdisk electrode | $4.90 \times 10^{-6}$ | $0.75 \times 10^{-6}$ | $5.5 \times 10^{-7}$ |
| 320 × 50 nm integrated SECM-AFM tips | $6.40 \times 10^{-10}$ | $1.37 \times 10^{-10}$ | $1.04 \times 10^{-10}$ |
| 700 × 50 nm integrated SECM-AFM tips | $1.40 \times 10^{-9}$ | $3.00 \times 10^{-10}$ | $2.30 \times 10^{-10}$ |
| 1700 × 50 nm integrated SECM-AFM tips | $3.40 \times 10^{-9}$ | $7.30 \times 10^{-10}$ | $5.5 \times 10^{-10}$ |

HCl buffer (0.1 mol L$^{-1}$, pH 7.2) was used as the supporting electrolyte. Specific sequence DNA for HCV type 1 (HCV-1, 18-mer) was custom-made by Integrated DNA Technologies, Inc (Coralville, IA). All chemicals were free of RNase and DNase and were used as received. The samples of target DNA (HCV-1, 2ac, 2b, and 3) from Hepatitis Health Service at Faculty of Pharmaceutical Sciences, Unesp, Brazil, were processed by the commercial assay Amplicor Hepatitis C Virus ver. 2.0 (Roche, USA). The concentration of DNA in the probe stock solutions was ~200 $\mu$g/mL; samples as well as diluted solutions were kept in a freezer. The sequences used in this study are summarized in Table 1.

**Apparatus.** Cyclic voltammetry (CV) and constant potential amperometry were performed using an electrochemical workstation (Autolab PGSTAT30, Eco Chemie, Utrecht, The Netherlands or 660A, CH Instruments Electrochemical, Austin, TX). All experiments were performed in a Faraday cage at room temperature (25 ± 1 °C). A three-electrode cell with a volume of 3 mL, comprising a 10-$\mu$m (Pt dual microdisk electrode) or a 25-$\mu$m (Pt microdisk electrode) diameter platinum working electrode (electroactive area: $7.90 \times 10^{-7}$ and $4.90 \times 10^{-6}$ cm$^2$, respectively), a Ag/AgCl reference electrode, and a platinum wire counter electrode was used for all electrochemical experiments. A detailed description of the microelectrode fabrication process is given elsewhere.[18] The integrated atomic force microscopy (AFM)-SECM tips (electrode edge length: 320, 700, and 1700 nm) were fabricated as previously described.[23] CV was performed using an electrochemical workstation (660A, CH Instruments Electrochemical) to characterize the microelectrodes, as well as submicro- and nanoelectrodes of integrated AFM-SECM tips. Ferrocenemethanol ($C_0$ = 2.0 mmol L$^{-1}$; $D = 7.8 \times 10^{-6}$ cm$^2$ s$^{-1}$)[24] was used during the characterization experiments. A typical sigmoidal shape of the voltammograms was obtained, corresponding well with the theory of microelectrodes. The actual radii of the Pt microelectrodes were $r = 5.0 \pm 0.2$ ($n = 3$) and $11.5 \pm 0.2$ $\mu$m ($n = 3$).

**Electropolymerization of Bilayer with Phosphonic Acid Tethers for DNA Immobilization.** The preparation of DNA microelectrodes based on layered polypyrrole/conducting 2,5-bis-(2-thienyl)-*N*-(3-phosphoryl-*n*-alkyl)pyrrole <pTPT**C3**-$PO_3H_2$ or pTPT**C11**-$PO_3H_2$> was performed according to a procedure described in detail elsewhere[19,18] using AcCN as solvent for pTPT**C3**-$PO_3H_2$ and a mixture of 60:40 dichloromethane/chloroform for pTPT**C11**-$PO_3H_2$, respectively. The PPy and pTPTC*n*-$PO_3H_2$ polymerization was controlled by chronocoulometry, and terminated once the total charge supplied by the electrode reached the values given in Table 2. CVs were recorded within a potential range of +0.3 to −0.3 V (vs Ag/AgCl at 0.05 V s$^{-1}$) in 0.1 mol L$^{-1}$ Tris-HCl buffer (pH 7.2). The specificity of DNA recognition was studied with synthetic 18-mer (specific sequence HCV type-1) oligonucleotide strands. The probe immobilization (18-mer: $1.0 \times 10^{-5}$ mol) was allowed to proceed for 5, 10, 20, 30, 40, 50, and 60 min. Again, CVs were recorded in 0.1 mol L$^{-1}$ Tris-HCl buffer (pH 7.2) after each incubation period.

**Detection of Hepatitis C Virus.** Target DNA was obtained by following procedure: the highly conserved 5′ noncoding region of HCV genome was amplified by nested reverse transcription PCR. The type-specific HCV-RNA viral load was determined by a quantitative assay (Cobas Amplicor HCV Monitor 2.0; Roche Diagnostics). The amplified products were then used in this study for the HCV RNA detection by the developed miniaturized label-free electrochemical genosensors. The PPy-pTPTC*n*-$PO_3H_2$-$Mg^{2+}$/HCV-1 DNA probe (18-mer: $1.0 \times 10^{-5}$ mol L$^{-1}$) modified

(22) (a) Hartung, J.; Kowalik, J.; Kranz, C.; Janata, J.; Josowicz, M.; Sinha, A.; McCoy, K. *J. Electrochem. Soc.* **2005**, *152*, E345−E350. (b) Aiyejorun, T.; Kowalik, J.; Janata, J.; Josowicz, M. J. *Chem. Educ.* **2006**, *83*, 1208−1211. (c) Kowalik, J.; Josowicz, M.; Janata, J. In *Towards Electrochemical Sensors for Genomics and Proteomics*; Palecek, E., Scheller, F., Wang, J., Eds.; Elsevier: New York, 2005.

(23) (a) Kranz, C.; Friedbacher, G.; Mizaikoff, B.; Lugstein, A.; Smoliner, J.; Bertagnolli, E. *Anal. Chem.* **2001**, *73*, 2491−2500. (b) Lugstein, A.; Bertagnolli, E.; Kranz, C.; Kueng, A.; Mizaikoff, B. *Appl. Phys. Lett.* **2002**, *81*, 349−351. (c) Lugstein, A.; Bertagnolli, E.; Kranz, C.; Kueng, A.; Mizaikoff, B. *Surf. Interface Anal.* **2002**, *33*, 146−150. (d) Kueng, A.; Kranz, C.; Mizaikoff, B.; Lugstein, A.; Bertagnolli, E. *Appl. Phys. Lett.* **2003**, *82*, 1592−1594. (e) Kueng, A.; Kranz, C.; Mizaikoff, B.; Lugstein, A.; Bertagnolli, E. *Angew. Chem., Int. Ed.* **2003**, *42*, 3238−3240.

(24) Miao, W. J.; Ding, Z. F.; Bard, A. J. *J. Phys. Chem. B* **2002**, *106*, 1392−1398.

electrodes were exposed to a solution of the mismatched oligonucleotides (244-mer HCV type 2a/c, 2b, and 3; individually; concentration $1.0 \times 10^{-15}$ mol $L^{-1}$) for 10 min at room temperature at gentle mixing. After washing, cyclic voltammograms were recorded evaluating any nonspecific interactions. In the following, the complementary interaction (244-mer HCV-1 DNA: $1.0 \times 10^{-23}$–$3.0 \times 10^{-15}$ mol $L^{-1}$) was performed at identically processed electrodes. The amplicon generated by the HCV DNA real-time Amplicor assay is located in a part of the HCV genome that has a relatively low melting temperature ($T_m$ = 55 °C in 50 mM NaCl). A low template melting temperature theoretically facilitates the annealing of primers and probes during PCR and during DNA hybridization steps. In order to further facilitate hybridization only for the perfectly matching sequences, more strict conditions—i.e., a higher temperature (37 °C)—should be investigated.

Prior to the electrochemical detection, all diluted samples were analyzed by the standard Amplicor Hepatitis C Virus Test, and the HCV-RNA viral load was determined at HCV RNA levels as low as $2.7 \times 10^{-18}$ mol $L^{-1}$ (detection limit of this method). After hybridization, the microelectrodes were thoroughly rinsed under stirring (5 min) in an excess of Tris-HCl buffer (pH 7.2), and cyclic voltammograms were again recorded. At low DNA concentrations, a smoothing algorithm was applied after each voltammetric measurement to reduce random noise and electromagnetic interference. The same procedure was applied to PPy-pTPT**C3**-$PO_3H_2$-$Mg^{2+}$/HCV-1 DNA probe (18-mer: $1.0 \times 10^{-9}$ mol) modified at submicro- and nanoelectrode-integrated AFM-SECM tips. An oligonucleotide sequence of the same length was used to evaluate complementary DNA binding (18-mer HCV-1 DNA: $1.0 \times 10^{-9}$ mol $L^{-1}$).

**Evaluation of DNA Hybridization through a Porous Polycarbonate Membrane.** In this study, a voltametric microbiosensor based on immobilization of the 18-mer HCV-1 DNA probe was applied in combination with SECM line scans to evaluate hybridization of DNA fragments diffusing through a porous polycarbonate membrane at physiologically relevant conditions. SECM line scans were performed with a home-built system as described elsewhere.[21] The electrochemical experiment was controlled by a bipotentiostat (CH Instruments 832A CH Instruments). A porous polycarbonate membrane (average pore size, 20 $\mu$m; Osmonics Inc., Minnetonka, MN) was mounted in a custom-built vertical diffusion cell separating a donor and a receptor compartment. All measurements were performed at room temperature using a three-electrode setup with an Ag/AgCl reference electrode, a platinum counter electrode, and either the bare platinum disk electrode or the PPy-pTPT**C3**-$PO_3H_2$-$Mg^{2+}$/ HCV-1 DNA probe (18-mer, $1.0 \times 10^{-9}$ mol $L^{-1}$) microbiosensor of the dual micoelectrode probe serving as the working electrode. The donor compartment contained complementary DNA solution (18-mer, $1.0 \times 10^{-9}$ mol $L^{-1}$).

In order to position the dual microelectrode in proximity to the membrane surface, the steady-state current at the unmodified platinum disk electrode was recorded as a function of the distance to the sample surface (*z*-approach curve). The change in Faraday current due to oxygen reduction at −520 mV versus Ag/AgCl was measured at the bare Pt microelectrode, as the tip was moved at a velocity of 2 $\mu$m/s in *z*-direction from the bulk solution toward the membrane separating the receptor and the donor compartment. After positioning of the dual microelectrode, SECM line scans were obtained by maintaining the tip at fixed *z*-position. Cyclic voltammograms in Tris-HCl buffer solution (pH 7.2) were recorded using the PPy-pTPT**C3**-$PO_3H_2$-$Mg^{2+}$/ HCV-1 DNA probe modified electrode. Following scanning in *x*-direction with a scan velocity of 4 $\mu$m/s, DNA hybridization was again evaluated by recording CVs in Tris-HCl buffer solution (pH 7.2).

## RESULTS AND DISCUSSION

**Detection of Hepatitis C Virus. (1) Effect of the Spacer Length of the pTPTC*n*-$PO_3H_2$ (*n* = 3 or 11) Layer.** In DNA biosensors, probes of single-stranded DNA of known sequence are immobilized at the transducer surface. When contacted with the sample solution, the DNA probes preferentially hybridize with free DNA targets incorporating the complementary sequence. For molecular diagnostics of human diseases, short ssDNA probes are usually terminally anchored or chemically grafted to solid surfaces. In the present label-free detection scheme for short-sequence (18- and 27-mer) DNAs, conducting modified polypyrrole films are deposited at a microelectrode surface. The addition of negative charges to the PPy-pTPT**C3**-$PO_3H_2$-$Mg^{2+}$/DNA probe modified electrode surface hinders chloride ion exchange due to phosphate acid groups of the complementary strand and results in a decrease in current of the recorded voltammogram, as previously reported.[18,19] Thereby, the hybridization of short DNA sequences could be determined with a limit of detection at 0.16 and 3.5 fmol (18- and 27-mer DNA targets, respectively).[18] The sensitivity of DNA biosensors and DNA microarrays is clearly dependent on the efficiency of hybridization at the surface. The efficiency of hybridization at the surface can be enhanced by increasing the distance (spacer length) between the DNA probes and the transducer surface, thus approaching hybridization conditions of free DNA probes in solution.

In the present study, PPy-pTPTC*n*-$PO_3H_2$-$Mg^{2+}$ microelectrode surfaces modified with oligonucleotide probes (18-mer) were used for detection of hepatitis C virus (HCV type 1), a clinically relevant analyte. In particular, the effect of the spacer length of the PPy-pTPTC*n*-$PO_3H_2$ (*n* = 3 or 11) on the hybridization event was investigated. Sterical flexibility can be added to the design of the sensor architecture by modifying the spacer length of the binding layer. Figure 1 shows the difference in obtained current values from the initial signal (PPy-pTPTC*n*-$PO_3H_2$-$Mg^{2+}$) to the current value obtained after probe immobilization (PPy-pTPTC*n*-$PO_3H_2$-$Mg^{2+}$/probe DNA) at 0.3 V in the cyclic voltammogram for two different linkers. A significant decrease of the current for the PPy-pTPTC*n*-$PO_3H_2$-$Mg^{2+}$ modified electrode after successive immersion in $1.0 \times 10^{-5}$ mol $L^{-1}$ HCV-1 DNA probe (18-mer) solution for 5, 10, 20, 30, 40, and 60 min was observed (Figure 1). After 20 min, the response of PPy-pTPT**C3**-$PO_3H_2$-$Mg^{2+}$/HCV-1 DNA probe was stabilized, indicating an effective immobilization of the 18-mer probe DNA at the PPy-pTPT**C3**-$PO_3H_2$-$Mg^{2+}$ film. Thus, a period of 30 min has been established as optimum period for probing DNA immobilization at the modified electrode surface. However, the incubation time for the 18-mer probe DNA immobilization at the PPy-pTPT**C11**-$PO_3H_2$-$Mg^{2+}$ film was significantly slower and completed only after 40 min of probe DNA incubation time. This behavior may be explained by the difference

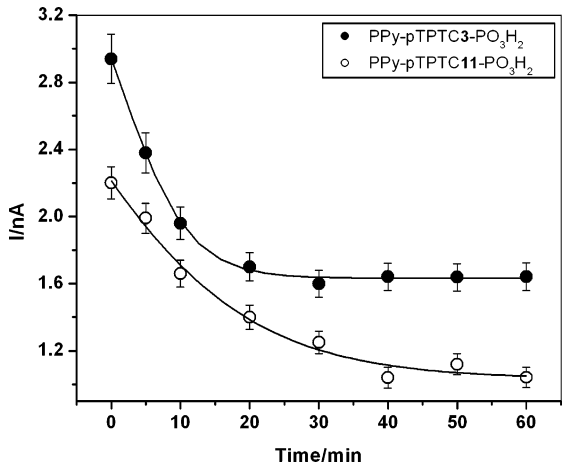


**Figure 1.** Effect of the incubation time of 18-mer DNA probe immobilized on PPy-pTPT**C3**$PO_3H_2$-$Mg^{2+}$ (•) and PPy-pTPT**C11**$PO_3H_2$-$Mg^{2+}$ (○) films ($n$ = 3).

in flexibility of the two spacers (C3 and C11, respectively) of the pTPTC$n$-$PO_3H_2$-$Mg^{2+}$ film. Hence, the orientation of bound biomolecules to the surface can be manipulated by the spacer length of the grafted layer. With longer spacers, bound biomolecules predominantly orient perpendicular to the surface, while at shorter spacers there is a more random distribution of orientations.[25] The maximal binding efficiency is obtained at a relatively low surface coverage of the spacer and with increased spacer chain length.

If the immobilized 18-mer probe DNA was incubated with a complementary DNA strand (244-mer HCV-1 DNA, $1.0 \times 10^{-15}$ mol $L^{-1}$), a significant change of the shape of the cyclic voltammogram was observed corresponding to a 27.2% decrease of signal in comparison to the signal derived from the cyclic voltammogram of the PPy-pTPT**C3**-$PO_3H_2$-$Mg^{2+}$/HCV-1 DNA probe prior to hybridization (Figure 2A) at the final potential (0.3 V) in the CV. The hybridization process was completed within 10 min, as previously decribed.[18] A higher decrease in response corresponding to 40.4% was obtained using PPy-pTPT**C11**-$PO_3H_2$-$Mg^{2+}$/ HCV-1 DNA probe (Figure 2B) after exposure of the modified electrode to the same concentration of HCV-1 DNA target solution (244-mer: $1.0 \times 10^{-15}$ mol $L^{-1}$). The hybridization events observed in Figure 2A and B can be also represented by subtraction of the complementary and noncomplementary interactions from the signal prior to hybridization (i.e., PPy-pTPTC$n$-$PO_3H_2$-$Mg^{2+}$/ HCV-1 DNA probe), as shown in Figure 2C. With variation of the spacer length (i.e., increased spacer length) from the polymer backbone, a higher sensitivity for target DNA molecules was obtained. It is hypothesized that the spacing between adjoining binding sites is smaller than the dimension of the ligands. If a certain number of consecutive binding sites are occupied with ligands in a cooperative manner using the C3 spacer, a neighboring binding site may be completely or partially blocked due to the steric crowding effect of bound ligands. Binding efficiency assays performed with PPy-pTPT**C11**$PO_3H_2$-$Mg^{2+}$ layers indicated that increasing the length of the linker increased the DNA hybridization efficiency. In order to use such genosensors in clinical settings, it is essential to minimize nonspecific binding leading to false positive response. Hence, control experiments with mismatched bases were performed (Figure 2, dashed line). No significant change of the CV in the presence of 244-mer strands from HCV genotype 2B (6-bp mismatched) was detected.

**(2) Specificity, Sensitivity, and Reproducibility of the DNA Sensor.** The ability of the -pTPTC$n$-$PO_3H_2$-$Mg^{2+}$/HCV-1 DNA probe to be sensitive to small variations in the sequence of nucleic acids is extremely important for the proposed application in clinical environments. The high degree of sequence heterogeneity found in HCV isolates requires particularly efficient and specific-sequence recognition. However, fabrication of robust probes capable of recognizing a wide range of isolates is a difficult task.[26] In this study, a HCV-1 capture probe (18-mer: 5′-CGC TCA ATG CCT GGA GAT-3′) was designed to hybridize to the 5′ untranslated region′, which is a highly conserved region of the hepatitis C virus genome for the determination of the HCV-1 genotype (244-mer DNA target: 5′-ATC TCC AGG CAT TGA GCG-3′). The specificity of the biosensor was evaluated by base mismatched DNA of the 244-mer specific sequences HCV type 2a/c (5-bp mismatched: 5′-AT**G** **G**CC **G**GG CAT **A**GA G**T**G-3′), 2b (6-bp mismatched: 5′-AT**G** **A**CC **GGA** CAT **A**GA G**T**G-3′), or 3 (4-bp mismatched: 5′-AT**T** T**C**T **G**GG **T**AT TGA GCG-3′). The location of mismatched nucleotides related to the capture probe varies depending on the heterogeneity at each position of the HCV-1 genome. Genetic heterogeneity is a hallmark of RNA viruses in general, and the hepatitis C virus (HCV) in particular, due to the lack of fidelity of viral RNA-dependent RNA polymerases.[27] In HCV, this genetic diversity has been organized into six major genotypes and over 80 subtypes. Isolates of the same genotype have an average DNA sequence identity of 95%, but different genotypes have on average DNA sequence identity close to 65%.[26] Therefore, the specificity of the -pTPTC$n$-$PO_3H_2$-$Mg^{2+}$/HCV-1 DNA probe is an important parameter for its applicability in clinical settings. For verification, all stock ($1.0 \times 10^{-15}$ mol $L^{-1}$) and diluted DNA solutions were analyzed by the standard Amplicor Hepatitis C Virus Test. The HCV-RNA viral load could be determined at HCV RNA levels as low as $2.7 \times 10^{-18}$ mol $L^{-1}$ with this method. The PPy-pTPTC$n$-$PO_3H_2$-$Mg^{2+}$/probe DNA film exhibited sufficient stability when stored in deionized water for 15, 30, and 90 min (Figure 3A) after the DNA incubation period. Furthermore, no significant change of the cyclic voltammogram in the presence of the mismatched sequences (244-mer HCV-2a/c, 2b, and 3: $1.0 \times 10^{-15}$ mol $L^{-1}$) was observed, as shown in Figure 3B. However, in the presence of the complementary HCV-1 DNA (244-mer: $1.0 \times 10^{-20}$ mol $L^{-1}$, Figure 3C), a significant change of the shape of the cyclic voltammogram was observed corresponding to a 12% signal decrease when compared to the signal derived from the cyclic voltammogram of the PPy-pTPTC$n$-$PO_3H_2$-$Mg^{2+}$/HCV-1 DNA probe prior to hybridization. The discrimination in hybridization between perfectly matched and bases-mismatched DNA duplexes relies on the stability of the newly formed double-stranded DNA, since the length of the complementary sequence, its GC base content, and the location of mismatched bases all

(25) Szleifer, I. *Bull. Am. Phys. Soc.* In press. ISSN: 0003−0503.

(26) Qiu, P.; Cai, X.-Y.; Wang, L.; Greene, J. R.; Malcolm, B. *BMC Microbiol.* **2002**, *2*, 1471−2180.

(27) (a) Grakoui, A.; McCourt, D. W.; Wychowski, C.; Feinstone, S. M.; Rice, C. M. *J. Virol.* **1993**, *67*, 2832−2843.

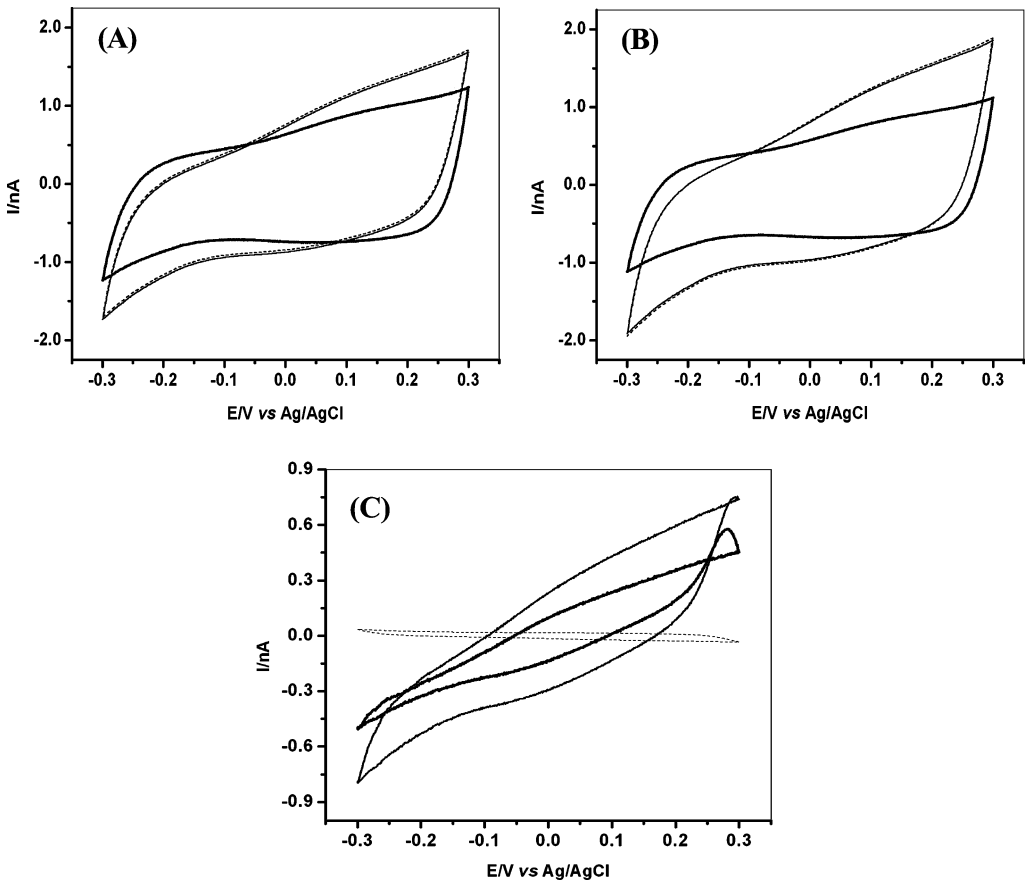


**Figure 2.** (A) Cyclic voltammograms recorded in 0.1 mol $L^{-1}$ Tris-HCl buffer pH 7.2 for the detection of DNA hybridization. (Light solid line) PPy-pTPT**C3**-$PO_3H_2$-$Mg^{2+}$/HCV-1 DNA probe; (dashed line) after exposure to $1.0 \times 10^{-15}$ mol $L^{-1}$ noncomplementary DNA; (dark solid line) same electrode after hybridization with DNA target ($1.0 \times 10^{-15}$ mol $L^{-1}$) for 10 min. (B) Cyclic voltammograms recorded in 0.1 mol $L^{-1}$ Tris-HCl buffer pH 7.2 for the detection of DNA hybridization: (light solid line) PPy-pTPT**C11**-$PO_3H_2$-$Mg^{2+}$/probe HCV-1 DNA; (dashed line) after exposure to $1.0 \times 10^{-15}$ mol $L^{-1}$ noncomplementary DNA; (dark solid line) same electrode after hybridization with DNA target ($1.0 \times 10^{-15}$ mol $L^{-1}$) for 10 min. (C) Results of subtraction of the cyclic voltammograms for the noncomplementary (dashed line) and complementary interactions from PPypTPT**C3**-$PO_3H_2$-$Mg^{2+}$/DNA probe (dark solid line) and PPypTPT**C11**-$PO_3H_2$-$Mg^{2+}$/HCV-1 DNA probe (light solid line) cyclic voltammograms. Scan rate, 0.05 V $s^{-1}$.

have strong effects on the duplex stability.[28] The addition of negative charges to the modified electrode surface due to phosphate groups of the complementary strand decreases the chloride ion-exchange rate leading to the current decrease in the observed CV. Thereby, the hybridization of the specific DNA sequence (DNA target) could be confirmed. Reproducibility studies were performed by comparing the hybridization signals obtained with the same concentration of complementary target oligonucleotides with different film depositions. For each surface, at least three replicate measurements were performed. The average hybridization value, standard deviation, and relative standard deviation obtained with the complementary target oligonucleotide are given in Table 3.

Figure 4 shows the logarithmic response as a function of the concentration of 244-mer target DNA. Each concentration was tested in three replicates ($n = 3$). The curve was plotted by averaging the values after subtraction of the response of the complementary interactions from the PPy-pTPTC*n*-$PO_3H_2$-$Mg^{2+}$/DNA probe. The sensitivity was derived from the slope of the fitted linear regression function at DNA concentrations of $2.57 \times 10^{-21}$ and $3.16 \times 10^{-22}$ mol $L^{-1}$ for PPy-pTPT**C3**-$PO_3H_2$ and PPy-pTPT**C11**-$PO_3H_2$, respectively. The background noise level was approximated by the average value of the signal at three points using mismatched sequence (244-mer) strands at the lowest concentration ($1.0 \times 10^{-9}$ mol $L^{-1}$). The background noise was determined to be $0.027 \pm 0.029$ (PPy-pTPT**C3**-$PO_3H_2$), and $0.035 \pm 0.04$ nA (PPy-pTPT**C11**-$PO_3H_2$). The limit of detection was determined at $3.71 \times 10^{-20}$ (PPy-pTPT**C3**-$PO_3H_2$) and $1.82 \times 10^{-21}$ mol $L^{-1}$ (PPy-pTPT**C11**-$PO_3H_2$). The 244-mer cDNA from HCV genotype 1 was obtained by reverse transcriptase-linked polymerase chain reaction.

**Detection of the DNA Hybridization Based on SECM-AFM Tip-Integrated DNA scensors.** Since the formation of the sensing layer is mainly based on electrochemical polymerization steps, the described DNA sensor can be further miniaturized and implemented into bifunctional AFM-SECM scanning probe tips with integrated electrodes in the submicrometer range. Figure 5 shows that a significant change of the shape of the cyclic voltammogram was observed corresponding to a 29.1% signal decrease when compared to the signal derived from the cyclic voltammogram of the PPy-pTPT**C3**-$PO_3H_2$-$Mg^{2+}$/HCV-1 DNA probe film after hybridization with DNA target (18-mer HCV-1

(28) Guo, Z.; Guilfoyle, R. A.; Thiel, A. J.; Wang, R.; Smith, L. M. *Nucleic Acids Res.* **1994**, *22*, 5456−5465.

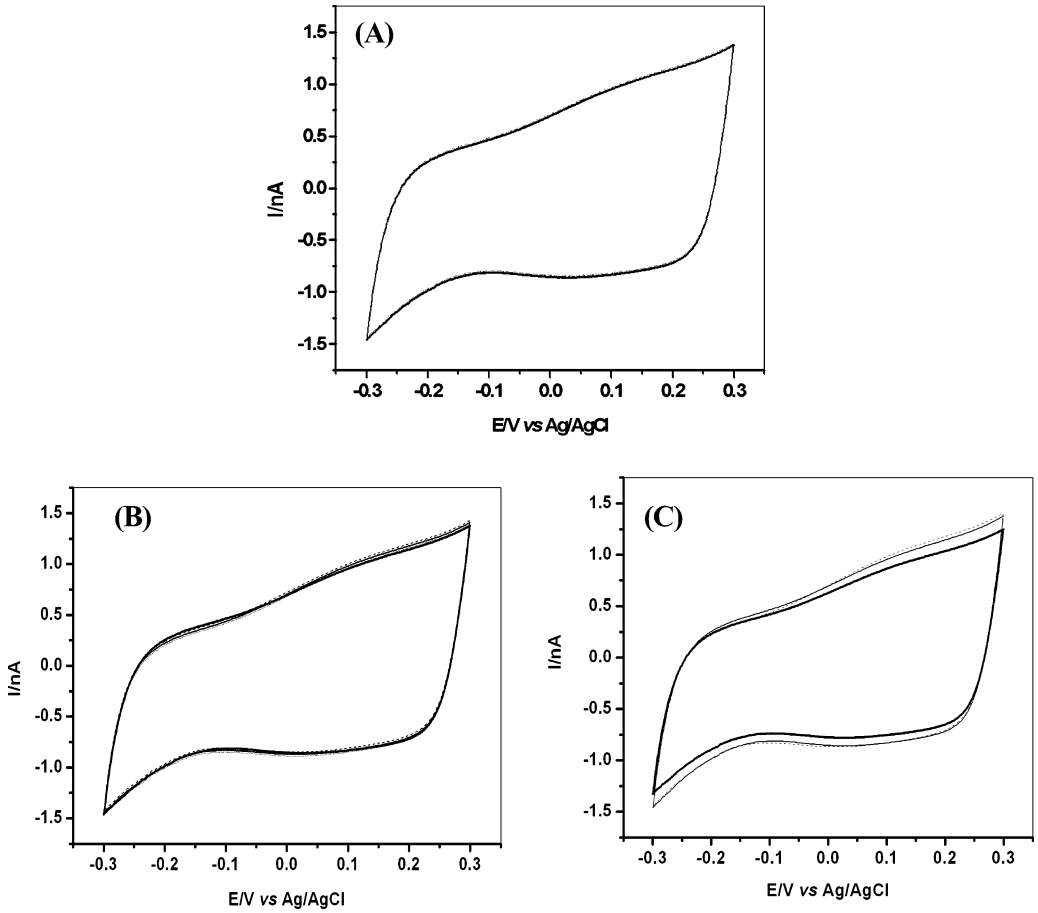


**Figure 3.** (A) Cyclic voltammograms recorded in Tris-HCl buffer (pH 7.2) at a PPy-pTPT**C11**-$PO_3H_2$-$Mg^{2+}$/probe DNA layer (dark solid line) and the same electrode after storage in deionized water for 15 (solid line), 30 (dashed line), and 90 (dotted line) min. (B) Cyclic voltammograms recorded in 0.1 mol $L^{-1}$ Tris-HCl buffer pH 7.2 for the detection of unspecific interactions: (dark solid line) PPy-pTPT**C11**-$PO_3H_2$-$Mg^{2+}$/HCV-1 DNA probe; after exposure to $1.0 \times 10^{-15}$ mol $L^{-1}$ noncomplementary (dashed line) HCV-2a/c DNA, (light solid line) HCV-2b DNA, and (dot solid line) HCV-3 DNA for 10 min. (C) Cyclic voltammograms recorded in 0.1 mol $L^{-1}$ Tris-HCl buffer pH 7.2 for the same electrode after hybridization with complementary HCV-1 DNA (244-mer, $1.0 \times 10^{-20}$ mol $L^{-1}$) for 10 min. Scan rate, 0.05 V $s^{-1}$.

**Table 3. Average Hybridization Value, Standard Deviation and Relative Standard Deviation Obtained with the PPy-pTPTC*n*-$PO_3H_2$-$Mg^{2+}$/HCV-1 DNA Probe Film after Exposure to DNA Target ($n = 3$)**

| | PPy-pTPTC3-$PO_3H_2$-$Mg^{2+}$/ HCV-1 DNA probe | | PPy-pTPTC11-$PO_3H_2$-$Mg^{2+}$/ HCV-1 DNA probe | |
|---|---|---|---|---|
| 244-mer HCV-1 DNA C/mol $L^{-1}$ | $I$/nA | RSD | $I$/nA | RSD |
| $1.0 \times 10^{-22}$ | $0.010 \pm 0.001$ | 10 | $0.010 \pm 0.001$ | 10 |
| $1.0 \times 10^{-20}$ | $0.130 \pm 0.01$ | 7.7 | $0.346 \pm 0.02$ | 5.8 |
| $1.0 \times 10^{-18}$ | $0.200 \pm 0.004$ | 2.0 | $0.651 \pm 0.01$ | 1.5 |
| $1.0 \times 10^{-15}$ | $0.457 \pm 0.01$ | 2.2 | $0.930 \pm 0.03$ | 3.2 |
| $3.0 \times 10^{-15}$ | $0.650 \pm 0.005$ | 1.0 | $1.00 \pm 0.01$ | 1.0 |

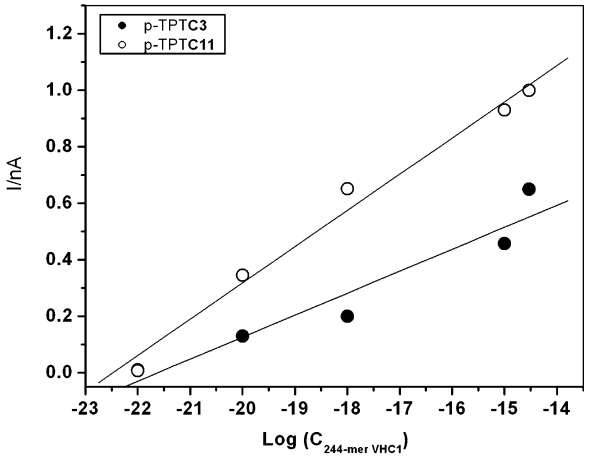


**Figure 4.** Calibration plot for the dependence of PPy-pTPTC*n*-$PO_3H_2$-$Mg^{2+}$/ HCV-1 DNA probe modified electrode response upon increasing the concentration of the 244-mer DNA target.

DNA, $1.0 \times 10^{-9}$ mol $L^{-1}$) for 10 min. No significant change of the cyclic voltammogram was detected in the presence of the mismatched sequences (18-mer HCV-2b DNA, $1.0 \times 10^{-9}$ mol $L^{-1}$).

**Detection of the DNA Hybridization through a Porous Polycarbonate Membrane.** SECM is an excellent tool for monitoring ionic or molecular transport through synthetic and biological porous membranes[29] and was applied for studying transport of DNA molecules through nanopores. This application is of interest when using nanopores for characterization/sequencing, separation, and sensing of DNA. In the present study, the hybridization of a short-sequence 18-mer DNA probe immobilized at the PPy-pTPT**C3**-$PO_3H_2$-$Mg^{2+}$ layer with 18-mer target oligonucleotides diffusing through a porous polycarbonate membrane

(29) Nagy, G.; Nagy, L. *Fresenius J. Anal. Chem.* **2000**, *366*, 735−744.

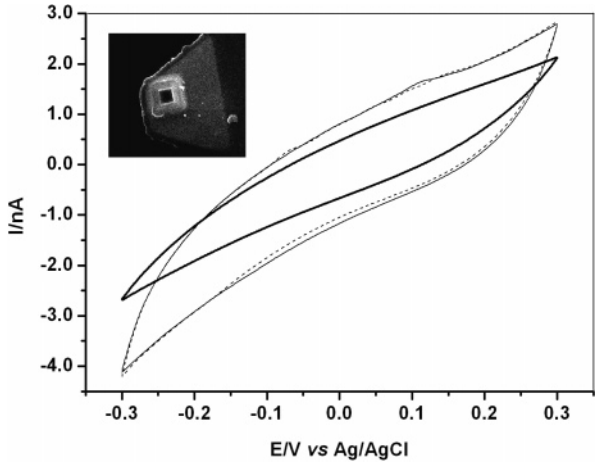


**Figure 5.** Cyclic voltammograms recorded in 0.1 mol $L^{-1}$ Tris-HCl buffer pH 7.2 for the detection of 18-mer DNA hybridization: (light solid line) PPy/pTPTC$_3$-PO$_3$H$_2$-Mg$^{2+}$/HCV-1 DNA probe; (dashed line) after exposure to 1.0 $\times$ $10^{-9}$ mol $L^{-1}$ noncomplementary DNA (HCV type 2b); (dark solid line) same electrode after hybridization with target HCV-1 DNA (18-mer, 1,0 $\times$ $10^{-9}$ mol $L^{-1}$) for 10 min. Scan rate was 0.05 V $s^{-1}$. SECM-AFM tip electrode.

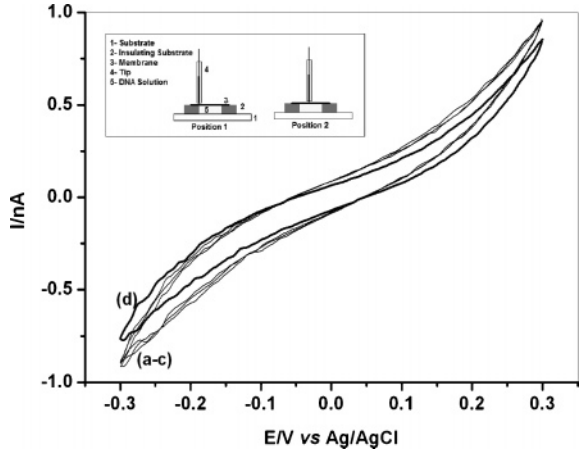


**Figure 6.** Cyclic voltammograms recorded in 0.1 mol $L^{-1}$ Tris-HCl buffer pH 7.2 Pt/tip electrode (conical electrode; diameter, 10 $\mu$m) modified with PPy/pTPTC$_3$-PO$_3$H$_2$-Mg$^{2+}$/HCV-1 DNA probe positioned to 300 $\mu$m (a), close to insulating substrate; (b) and close to poretic membrane (interface of DNA target solution: 18-mer HCV-1 DNA, 1,0 $\times$ $10^{-9}$ mol $L^{-1}$) after 0, (c) 5, and (d, —) 10 min of incubation time.

was investigated. The hybridization event was evaluated after positioning the microbiosensor via SECM *z*-approach curves recorded using a 10-$\mu$m-diameter dual microdisk electrode assembly. The unmodified Pt disk microelectrode was biased at a potential of −520 mV versus Ag/AgCl, which governs the diffusion-controlled reduction of molecular oxygen in air-saturated phosphate-buffered saline solution. As the microelectrode assembly is approaching the surface of the insulating polycarbonate membrane, hemispherical diffusion of the oxygen toward the microelectrode surface is blocked (negative feedback effect) resulting in a decrease of the steady-state current ($i_{W1}$) measured at the microelectrode compared to the steady-state current in bulk solution ($i_{W1}$, ∞). The resulting approach curves provide the normalized tip current ($i_{W1}/i_{W1}$, ∞) in dependence of the distance *d* between tip and substrate.[30] The real-time dynamic process of the hybridization was monitored by recording CVs in Tris-HCl buffer solution (pH 7.2) at different times, as shown in Figure 6. Cyclic voltammograms were recorded in 0.1 mol $L^{-1}$ Tris-HCl buffer (pH 7.2) with PPy/pTPTC$_3$-PO$_3$H$_2$-Mg$^{2+}$/DNA probe (18-mer HCV-1 DNA, 1.0 $\times$ $10^{-9}$ mol $L^{-1}$) at modified disk electrodes positioned close to insulating substrate (Figure 6, position 1, curve a). In the following, the dual electrode was scanned in the *x*-direction at constant height with a scan velocity of 4 $\mu$m/s for positioning the modified disk electrode onto porous membrane/DNA target solution (18-mer HCV-1 DNA: 1.0 $\times$ $10^{-9}$ mol $L^{-1}$, Figure 6, position 2, curve b). Cyclic voltammograms were recorded in 0.1 mol $L^{-1}$ Tris-HCl buffer at pH 7.2 after 5 (curve c) and 10 (curve d) min. The biosensor exhibited rapid hybridization with target DNA (18-mer HCV-1 DNA, 1.0 $\times$ $10^{-9}$ mol $L^{-1}$). A significant decrease in the CV was observed, and the hybridization process was completed within 10 min (Figure 6, curve d). Therefore, it is concluded that SECM could be used for localized detection of DNA diffusing through porous membrane or channels via the label-free hybridization scheme presented in this study. It is anticipated that the detection process can be accelerated by further optimizing the hybridization conditions such as, for example, salt concentration and temperature. The performance of the miniaturized genosensor system revealed sufficient specificity and reproducibility of DNA hybridization events and has significant potential for AFM-SECM tip-integrated DNA nanoassay technology in the future enabling combined AFM-SECM experiments for monitoring localized sources of DNA, e.g., at biological surfaces and interfaces via precise genosensor positioning.

## CONCLUSIONS

A label-free detection scheme for short (18-mer) and long (244-mer) DNA sequences detecting HCV-1 DNA based on conducting polypyrrole modified films deposited onto microelectrode surfaces is reported. The addition of negative charges to the PPy-pTPTC$_3$-PO$_3$H$_2$-Mg$^{2+}$/DNA probe modified electrode surface due to phosphate groups of the complementary strand further hinders chloride ion exchange and causes a decrease in measured current during cyclic voltammetry. Furthermore, it was demonstrated that varying the spacer length from the polymer backbone affects the sensitivity of DNA target molecule detection and that rapid detection of 244-mer HCV-1 DNA sequences is possible at ultratrace levels. The performance of the miniaturized genosensor system revealed excellent reproducibility and selectivity of DNA hybridization events. In particular, HCV-1 DNA detection did not show unspecific interactions in the presence of mismatched sequences from 244-mer HCV-2a/c, 2b, and 3. Moreover, the label-free electrochemical biosensor allowed the detection of HCV-1 with a detection limit of 1.82 $\times$ $10^{-21}$ mol $L^{-1}$. For 18-mer target DNA, the applicability of this detection scheme at micrometer-sized electrodes and submicro- and nanoelectrodes integrated into AFM-SECM tips with high specificity, reproducibility, and rapid response to hybridization events was also demonstrated. Finally, short-sequence (18-mer) target DNA was also detected after diffusion through a porous polycarbonate membrane utilizing SECM

(30) Mirkin, M. V.; Horrocks, B. R. *Anal. Chim. Acta* **2000**, *406*, 119−146.

positioning of the microgenosensor, which enables highly localized DNA detection.

## ACKNOWLEDGMENT

B.M. and C.K. gratefully acknowledge financial support from the National Institutes of Health (EB000508), M.J. from the Georgia Research Alliance, and C.d.S.R. and H.Y. from the Brazilian Founding Agency FAPESP. J.K. acknowledges partial funding from the U.S. Department of Energy.

Received for review July 31, 2007. Accepted October 6, 2007.

AC701613T